

On measuring the absolute scale of baryon acoustic oscillations

Will Sutherland^{1*}

¹*School of Physics and Astronomy, Queen Mary University of London, Mile End Road, London E1 4NS*

MNRAS - Accepted 2012 July 5. Received 2012 July 5; in original form 2012 May 3

ABSTRACT

The baryon acoustic oscillation (BAO) feature in the distribution of galaxies provides a fundamental standard ruler which is widely used to constrain cosmological parameters. In most analyses, the comoving length of the ruler is inferred from a combination of CMB observations and theory. However, this inferred length may be biased by various non-standard effects in early universe physics; this can lead to biased inferences of cosmological parameters such as H_0 , Ω_m and w , so it would be valuable to measure the *absolute* BAO length by combining a galaxy redshift survey and a suitable direct low- z distance measurement. One obstacle is that low-redshift BAO surveys mainly constrain the ratio $r_S/D_V(z)$, where D_V is a dilation scale which is not directly observable by standard candles. Here, we find a new approximation $D_V(z) \simeq \frac{3}{4}D_L(\frac{4}{3}z)(1 + \frac{4}{3}z)^{-1}(1 - 0.02455z^3 + 0.0105z^4)$ which connects D_V to the standard luminosity distance D_L at a somewhat higher redshift; this is shown to be very accurate (relative error < 0.2 percent) for all WMAP-compatible Friedmann models at $z < 0.4$, with very weak dependence on cosmological parameters H_0 , Ω_m , Ω_k , w . This provides a route to measure the absolute BAO length using only observations at $z \lesssim 0.3$, including type-Ia supernovae, and potentially future H_0 -free physical distance indicators such as gravitational lenses or gravitational wave standard sirens. This would provide a *zero-parameter* check of the standard cosmology at $10^3 \lesssim z \lesssim 10^5$, and can constrain the number of relativistic species N_{eff} with fewer degeneracies than the CMB.

Key words: cosmology: large-scale structure of Universe – cosmic microwave background – distance scale.

1 INTRODUCTION

The detection of baryon acoustic oscillations (BAOs) in the large-scale distribution of galaxies in both the SDSS (Eisenstein et al 2005) and 2dFGRS (Cole et al 2005) redshift surveys was a triumph for the standard cosmological model; the BAO feature (Peebles & Yu 1970; Bond & Efstathiou 1984; Eisenstein & Hu 1998; Meiksin, White & Peacock 1999) is essentially created by closely related physics to the acoustic peaks in the cosmic microwave background (CMB) temperature power spectrum. Therefore, the observed BAO feature supports the standard cosmology in several independent ways: the existence of the feature supports the basic gravitational instability paradigm for structure formation; the relative weakness of the BAO feature supports the $\sim 1 : 5$ ratio of baryons to dark matter, since a baryon-dominated universe would

have a BAO feature much stronger than observed; and the observed length-scale of the feature in redshift space is consistent with the concordance Λ CDM model derived from the CMB and other observations, with $\Omega_m \approx 0.27$ and $H_0 \approx 70 \text{ km s}^{-1} \text{ Mpc}^{-1}$ (Komatsu et al 2011).

Recently, there have been several new independent measurements of the BAO feature in galaxy redshift surveys, e.g. from SDSS-DR8 (Percival et al 2010), WiggleZ (Blake et al 2011), 6dFGRS (Beutler et al 2011), and an angular measurement from SDSS-DR9 (Seo et al 2012), which are all consistent with the concordance Λ CDM model at the few-percent level.

The BAO feature is probably the best-understood standard ruler in the moderate-redshift Universe, and therefore in conjunction with CMB observations it offers great power for constraining cosmological parameters including dark energy (Weinberg et al 2012). A number of theoretical and numerical studies (Seo et al 2008, 2010) have concluded that the comoving length-scale of the BAO feature evolves by

* E-mail: w.j.sutherland@qmul.ac.uk

~ 0.5 percent between the CMB era and $z \sim 0.3$ due to non-linear growth of structure, but this shift can be corrected to the 0.1 percent level using reconstruction methods (Padmanabhan et al 2012). Therefore, there are several very ambitious redshift surveys including the ongoing WiggleZ (Blake et al 2011), BOSS (White et al 2011) and HETDEX, the recently approved ESA Euclid space mission (Laureijs et al 2011), and the proposed BigBOSS and WFIRST, which plan to survey $\sim 1 - 50$ million galaxy redshifts over huge volumes, to give sub-percent measurements of the BAO feature at various redshifts $0.2 \lesssim z \lesssim 2.5$.

However, one drawback of the BAO feature is that the comoving length $r_s(z_d)$ is calibrated at $z > 1000$ using a combination of CMB observations and theory; this leaves us vulnerable to systematic errors from possible unknown new physics at early times (see §2 for discussion). Low-redshift measurements of the BAO scale essentially measure a ratio of r_s relative to some distance which is itself dependent on cosmological parameters H_0, Ω_m, w etc. Therefore, in a joint fit to CMB+BAO data, a wrong assumption in the CMB measurement of r_s may be masked by biased values of cosmological parameters, i.e. a “precisely wrong” outcome (see §4 for an example).

In this letter we present a new and useful approximation which can accurately anchor the absolute BAO lengthscale using only low redshift measurements at $z \lesssim 0.3$, therefore providing a clean zero-parameter test of the standard early-universe cosmology, in particular the density of relativistic particles.

The plan of the paper is as follows: in § 2 we briefly review the main features of BAO observations, then in § 3 we present the new approximation for the dilation scale $D_V(z)$. In § 4 we review the effects of non-standard radiation density, and in § 5 we discuss potential observational issues for measuring the absolute BAO length. We summarise our conclusions in § 6.

Throughout the paper we use the standard notation that Ω_i is the present-day density of species i relative to the critical density; and the physical density $\omega_i \equiv \Omega_i h^2$, with $h \equiv H_0 / (100 \text{ km s}^{-1} \text{ Mpc}^{-1})$. Our default model is flat Λ CDM with $\Omega_m = 0.27$; in other cases, w is the dark energy equation of state, $\Omega_{tot} = \Omega_m + \Omega_\Lambda$ is the total density parameter, and $\Omega_k \equiv 1 - \Omega_{tot}$.

2 OBSERVATIONS OF THE BAO LENGTH

The BAO feature appears as a single hump in the galaxy correlation function $\xi(r)$, or equivalently a series of decaying wiggles in the power spectrum (see Eisenstein, Seo & White (2007b) for a clear exposition, and Bassett & Hlozek (2010) for a recent review). In the following, we denote r_s to be the comoving length scale of the BAO feature in a galaxy redshift survey, while $r_s(z_d)$ is the comoving sound horizon at the baryon drag epoch $z_d \approx 1020$, which is conventionally defined as the fitting formula Eq. 4 of Eisenstein & Hu (1998). These lengths are not quite identical due to evolution of perturbations after the drag epoch and non-linear growth of structure, but the shifts are predicted to be below the 0.6 percent level and well correctable from theory (Eisenstein et al 2007a; Seo et al 2008, 2010); therefore,

measuring the BAO feature at low redshift provides a very robust link to the sound horizon in the CMB era.

In the small angle approximation and assuming we observe a redshift shell which is thin compared with its mean redshift, the angular size of the BAO feature is $\Delta\theta(z) = r_s / (1+z) D_A(z)$, where $D_A(z)$ is the usual proper angular-diameter distance to redshift z ; and the difference in redshift along one BAO length in the line-of-sight direction is $\Delta z_{\parallel}(z) = r_s H(z) / c$ (Blake & Glazebrook 2003; Seo & Eisenstein 2003)

In practice, current galaxy redshift surveys are not quite large enough to distinguish the BAO feature separately in angular and radial directions, so the current measurements constrain a spherically-averaged length scale; the most model-independent quantity derived from these observations is $r_s / D_V(z)$, where D_V is called the dilation scale and is defined by Eisenstein et al (2005) as

$$D_V(z) \equiv \left[(1+z)^2 D_A^2(z) \frac{cz}{H(z)} \right]^{1/3} \quad (1)$$

This is essentially a geometric mean of two transverse and one radial directions.

Measuring the BAO feature from a galaxy redshift survey requires a mapping from observed galaxy positions and redshifts to galaxy pair separations in comoving coordinates, which is itself dependent on cosmological parameters including H_0, Ω_m, w etc. Therefore, extracting the value of r_s from a galaxy redshift survey is slightly theory-dependent; but the above dimensionless ratios $\Delta\theta(z)$, $\Delta z_{\parallel}(z)$ and $r_s / D_V(z)$ are essentially theory-independent, since to first order any change in the reference cosmology produces an equal shift in the fitted length r_s .

As above, the comoving length $r_s(z_d)$ is defined as the sound horizon at the baryon drag epoch $z_d \approx 1020$ (Eisenstein & Hu 1998). Adopting standard early-universe assumptions, $r_s(z_d)$ depends only on the densities of matter, baryons and radiation; the latter is very well constrained by the CMB temperature (assuming standard neutrino content), hence r_s depends only on ω_m and ω_b , which in turn are well constrained by the heights and morphology of the first three CMB peaks. Fits from the WMAP7 data alone (Komatsu et al 2011) give $r_s(z_d) \approx 153 \text{ Mpc}$ with approximately 1.3 percent precision, and forthcoming data from the Planck mission (Ade et al 2011) is expected to improve this prediction of r_s to ≈ 0.3 percent precision.

We note that the CMB derivation of $r_s(z_d)$ does not rely on assuming a flat universe or details of dark energy, since the observed CMB peak heights constrain ω_m and ω_b well without assuming flatness. However, the inference of $r_s(z_d)$ does rely on many simple but weakly tested assumptions about the $z > 1000$ universe, including

- (i) Standard GR,
- (ii) Standard radiation content (photons plus an effective number $N_{\text{eff}} \approx 3.04$ light neutrinos),
- (iii) Standard recombination history, including negligible variation in fundamental constants.
- (iv) Negligible early dark energy,
- (v) Negligible contribution of isocurvature fluctuations,
- (vi) The primordial power spectrum is smooth and almost a power-law.
- (vii) Densities of matter and radiation scale as the stan-

standard powers of scale factor; e.g. negligible late-decaying particles at $z \lesssim 10^6$ etc.

If one or more of the above assumptions are wrong, this can bias the value of r_s deduced from the CMB fits, and in turn this will generally result in biased inferences about other cosmological parameters (especially H_0) when doing joint fits to CMB and BAO data. Possible violation of (ii) above was analysed by Eisenstein & White (2004), and is discussed later in § 4; for some other non-standard cases, see for example Linder & Robbers (2008) for early dark energy, Menegoni et al (2012) for varying α , and Zunckel et al (2011) for the effect of isocurvature fluctuations.

For the above reasons, measuring the *absolute* BAO length scale at low redshift forms a powerful consistency test of the assumptions underlying standard cosmology at $z > 1000$.

The well-known route to this is to measure the transverse BAO scale at some effective redshift which gives $r_s/(1+z)D_A(z)$, and also use a combination of standard candles (e.g. SNe Ia) and the local Hubble constant H_0 to measure the usual luminosity distance, $D_L(z)$, to the same redshift. Combined with the standard distance-duality relation $D_L(z) = (1+z)^2 D_A(z)$, this can give a theory-independent absolute measurement of the BAO length. However, one disadvantage of the above is that it requires a BAO survey of sufficiently large volume to separate the transverse and radial BAO scales, and reaching sufficient cosmic volume requires a survey at significant redshift $z \gtrsim 0.3$; in turn, this means that type-Ia SNe are likely the only distance indicators bright enough to be useful for measuring $D_L(z)$, and there is a non-negligible time baseline over which supernova evolution may bias the measurements of $D_L(z)$.

As a complement to the above, it would be valuable to calibrate r_s using BAO measurements of $r_s/D_V(z)$ at lower redshifts $0.1 \lesssim z \lesssim 0.25$, combined with an accurate calibration of $D_V(z)$ from distance indicators. Although BAO surveys at lower redshift suffer from increased cosmic variance due to the limited available volume, there are several compensating benefits: there is a shorter time baseline for possible evolution of SNe properties; the SNe are brighter and more readily observable in the rest-frame near-IR; and low redshift offers better prospects for using alternative distance indicators such as gravitational lens time-delays, and potentially gravitational-wave standard sirens (Sathyaprakash et al 2011); and finally we avoid the complication of separating the radial and angular BAO scales in the analysis.

However, this low- z route requires an absolute measurement of $D_V(z)$ rather than $D_A(z)$, which is slightly more challenging; from Eq. 1, a measurement of $D_L(z)$ tells us $D_V(z)$ apart from an unknown factor of $H(z)^{1/3}$; this is helpful due to the $1/3$ power of H , but is not good enough for percent-level precision. At $z \rightarrow 0$, $D_V(z) \rightarrow cz/H_0$ as with all cosmological distances; however, there is insufficient volume to measure the BAO feature at $z \lesssim 0.05$, while beyond this cosmological distance effects cannot be ignored. For a concordance Λ CDM model at an example $z = 0.2$, the crude approximation $D_V(z) \sim cz/H_0$ is 6 percent too large, while the approximation $D_V(z) \approx D_L(z)/(1+z)$ is too large by 1.6 percent; these approximations are clearly not good enough for precision cosmology.

Since $D_V(z)$ is directly related to the comoving volume element per unit redshift, via

$$\frac{dV_c}{dA dz} = \frac{c(1+z)^2 D_A^2(z)}{H(z)} = \frac{1}{z} D_V^3(z) \quad (2)$$

where dV_c is comoving volume and dA is solid angle, we could measure D_V directly if we could observe a population of “standard counters” of known comoving number density. Unfortunately, our limited understanding of galaxy evolution implies that there is little hope of finding standard counters good enough for a percent-level measurement of D_V . Alternatively, a direct measurement of $H(z)$ is possible using differential ages of red galaxies (e.g. Stern et al 2010), but again it may be very challenging to reach few-percent absolute accuracy with this method.

In the next Section, we show a new alternative route for obtaining accurate calibration of D_V : we find a much better approximation for D_V , which relates $D_V(z)$ to the observable D_L at a slightly higher redshift, specifically $\frac{4}{3}z$.

3 A ROUTE TO MEASURING D_V

3.1 Relation between D_V and D_L

Here we find an accurate approximation relating the dilation length $D_V(z)$ to the observable luminosity distance D_L at a slightly higher redshift.

We first define as usual the scale factor $a \equiv (1+z)^{-1}$ with $a_0 = 1$, and the time-dependent Hubble parameter $H(z) = \dot{a}/a$ where dot denotes time derivative. We also have the usual expression for comoving radial distance,

$$D_R(z_1) = c \int_0^{z_1} \frac{1}{H(z)} dz \quad (3)$$

In the Appendix of Sutherland (2012), we found a good approximation at moderate redshift

$$D_R(z) \approx \frac{cz}{H(\frac{2}{3}z)}, \quad (4)$$

This approximation was derived using a Taylor-series expansion of $1/H(z)$ around redshift $z/2$; this results in the first derivative $(1/H)'$ cancelling so there is no error of order z^2 , and uses the convenient fact that the second derivative $(1/H)''$ has a zero-crossing at $z \sim 0.3$ in a concordance Λ CDM model, so the error of order z^3 is small at moderate redshift. In a flat universe this leads to

$$D_L(z) \approx (1+z) \frac{cz}{H(\frac{2}{3}z)}. \quad (5)$$

This is still fairly accurate even for weakly-curved models, since the multiplicative change in D_L for a non-flat model is of order $1 + \Omega_k z^2/6$ for fixed expansion history; for plausible values of $|\Omega_k| < 0.05$, this is a very small effect at $z \lesssim 0.3$.

In Sutherland (2012) we also found a good approximation for $D_V(z)$ at moderate redshift, which is

$$D_V(z) \approx \frac{cz}{H(\frac{2}{3}z)} \quad (6)$$

Both approximations (5) and (6) are accurate to ≤ 0.4 percent for $z < 0.5$ for models reasonably close to standard Λ CDM; the error in approximation (6) is shown in Figure 1 for some example models. (This will be useful below in § 4.3).

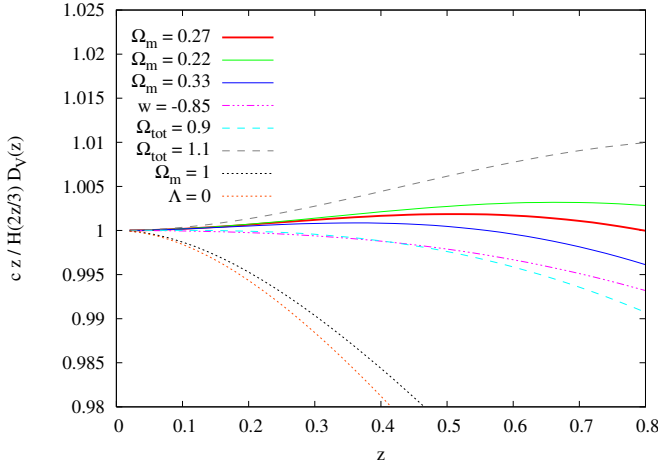


Figure 1. This figure shows the relative accuracy of approximation 6 for various cosmological models. The solid lines show flat Λ CDM models with $\Omega_m = 0.22, 0.27, 0.33$ (top to bottom). The dashed lines show non-flat Λ CDM with $\Omega_{tot} = 0.90$ (lower) and 1.1 (upper). The dash-dot line shows flat w CDM with $w = -0.85$. The dotted lines show $\Omega_m = 1$ (upper), and open $\Omega_m = 0.27, \Omega_\Lambda = 0$ (lower).

Both Eqs. 5 and 6 involve $H(z)$ at slightly different redshifts; however, it is clear from the above that if we consider a BAO measurement at effective redshift z_1 , then $D_V(z_1)$ is closely related to $H(2z_1/3)$, while if we consider $D_L(4z_1/3)$ this is also related to $H(2z_1/3)$; we can therefore combine approximations 5 and 6 to cancel the unknown $H(2z_1/3)$, which gives the approximation

$$D_V(z) \simeq \frac{3}{4} D_L \left(\frac{4}{3} z \right) \left(1 + \frac{4}{3} z \right)^{-1}. \quad (7)$$

We now explore the error in approximation 7: Figure 2 shows the ratio of the RHS of Eq. 7 to the exact $D_V(z)$ for various example cosmological models. Unless otherwise specified, we take $\Omega_m = 0.27$ for each model. Specifically, Figure 2 shows three flat Λ CDM models with $\Omega_m = 0.22, 0.27, 0.33$; one flat w CDM model with $w = -0.85$; and two non-flat Λ CDM models with $\Omega_{tot} = 0.9$ and 1.1 respectively; finally, an Einstein-de Sitter $\Omega_m = 1$ model, and a zero dark energy model with $\Omega_m = 0.27, \Omega_\Lambda = 0$. (These latter two models are well known to be grossly inconsistent with CMB and other measurements, but are included for comparison purposes).

It is clear from Figure 2 that approximation 7 is surprisingly accurate: for the three Λ CDM models the error is less than 0.2 percent at $z < 0.4$, and the w CDM model is only slightly worse. The two Λ CDM models are still quite good, with error < 0.4 percent at $z < 0.4$; this is considerably better than the medium-term expected errors ~ 1 percent on the BAO ratio, and also current upper limits on $|\Omega_k|$ are significantly tighter than 0.1; more realistic values $|\Omega_k| \sim 0.02$ give rise to minimal error in (7). Therefore for any WMAP-allowed model, the error in approximation (7) is several times smaller than the medium-term precision on BAO observables.

The approximation 7 becomes significantly worse for the Einstein-de Sitter and open zero- Λ models, with errors

respectively +1.25 percent and +2.0 percent at $z = 0.4$; however, even these give sub-percent error at $z \leq 0.25$.

In fact, Eq. (7) is exact at all z for a de Sitter model with $\Omega_m = 0, \Omega_\Lambda = 1$, while its accuracy degrades rather slowly with increasing Ω_m and/or curvature; thus, for near-flat and accelerating models favoured by current data, it is remarkably accurate. An explanation of this property in terms of Taylor series is given in Appendix A: this shows that (7) is exact to second order in z independent of all cosmological parameters; while at third order, there is a fortunate coincidence that for deceleration parameter $q_0 \lesssim -0.4$ and small curvature, the difference in the z^3 coefficients is also small. This makes Eq. 7 accurate at $z \lesssim 0.4$ for all near-flat accelerating models, with little dependence on precise values of Ω_m, Ω_k, w etc. (Note that all results in the main body of the paper use the numerical integrals for D_V and D_L ; the Taylor series in Appendix A are only provided as an aid to intuition).

We also see from Figure 2 that approximation (7) is a slight overestimate of the exact $D_V(z)$ for all the flat and open models shown; only the closed model ($\Omega_{tot} = 1.1$) gives an underestimate. Since (7) gives a slight overestimate of the exact D_V for all the plausible models fairly close to Λ CDM, we can get a modest but useful improvement by removing this bias, by multiplying by a polynomial in z chosen to give a good fit for concordance Λ CDM; we find an excellent fit with small terms in z^3 and z^4 , specifically

$$D_V(z) \simeq \frac{3}{4} D_L \left(\frac{4}{3} z \right) \left(1 + \frac{4}{3} z \right)^{-1} (1 - 0.0245 z^3 + 0.0105 z^4). \quad (8)$$

By construction, this approximation is excellent for the concordance model, with relative error < 0.02 percent at $z \leq 1$. For other plausible models, the resulting ratio (RHS of 8) / (exact $D_V(z)$) is shown in Figure 3; in this Figure we have used a smaller range of Ω_k for the non-flat models, and added two models with time-varying w with the common parametrisation $w(a) = w_0 + w_a(1 - a)$, to give a set of models roughly spanning the 2σ allowed range from current data.

It is clear from Figure 3 that approximation 8 is very accurate in the WMAP-allowed neighbourhood of Λ CDM, including generous variations of Ω_m , modest curvature and $w \neq -1$. For all the models shown the relative error is smaller than $(z/200)$ at $z < 1$, thus 0.2 percent error at $z \leq 0.4$. This error is substantially smaller than the cosmic variance in BAO measurements, and the expected accuracy in next-decade absolute distance measurements, so is almost negligible for practical measurements of r_s .

This means that a direct measurement of $D_L(4z/3)$ can immediately predict $D_V(z)$ with very little dependence on cosmological parameters $H_0, \Omega_m, \Omega_k, w$. Multiplying this by a BAO measurement of $r_s/D_V(z)$ from a galaxy redshift survey thus measures r_s in comoving Mpc, based entirely on low-redshift data.

This can then be compared with a CMB-only prediction of $r_s(z_d)$ for a *zero parameter* test of our early universe assumptions: if the local r_s measured from BAOs and D_L as above is not consistent with the r_s inferred from the CMB, something is definitely wrong with one or more measurements, or the early-universe assumptions or the FRW framework; tuning of the late-time cosmological parameters Ω_m, Ω_k, w within the 3σ WMAP-allowed ranges cannot sig-

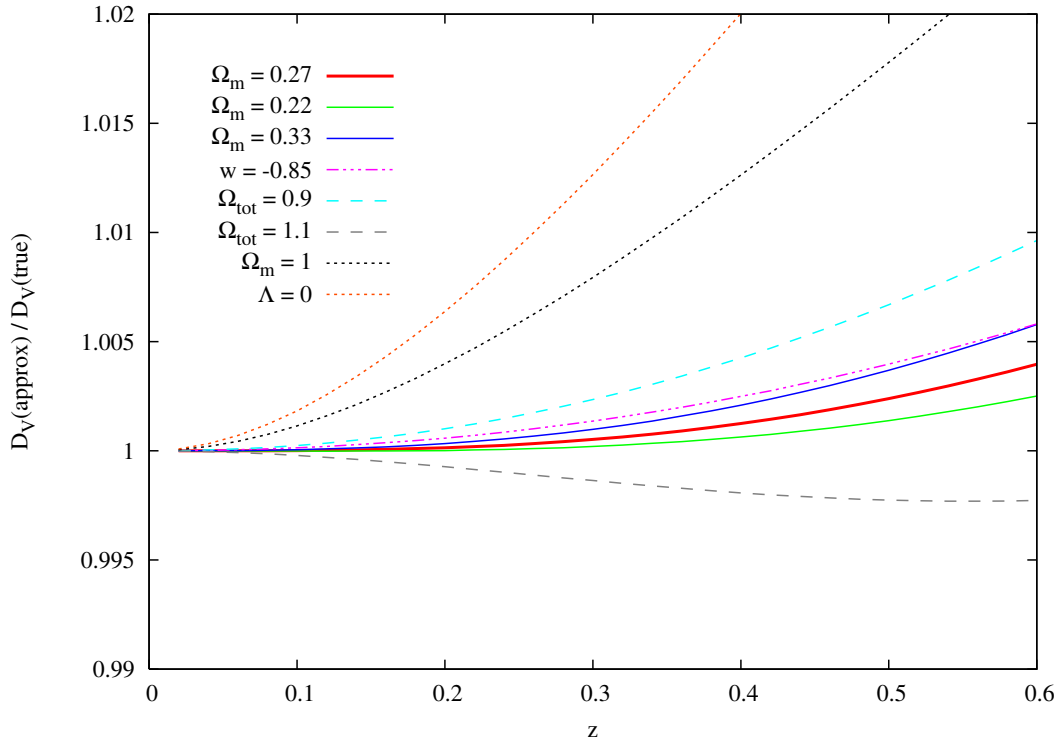


Figure 2. This figure shows the relative accuracy of approximation 7 for the same models as Figure 1. The three solid lines show flat Λ CDM models with $\Omega_m = 0.22, 0.27, 0.33$ (bottom to top). The dashed lines show non-flat Λ CDM with $\Omega_{tot} = 0.90$ (upper) and 1.1 (lower). The dot-dash line shows flat w CDM with $w = -0.85$. The dotted lines show $\Omega_m = 1$ Einstein-de Sitter (lower) and open $\Omega_m = 0.27, \Omega_\Lambda = 0$ (upper).

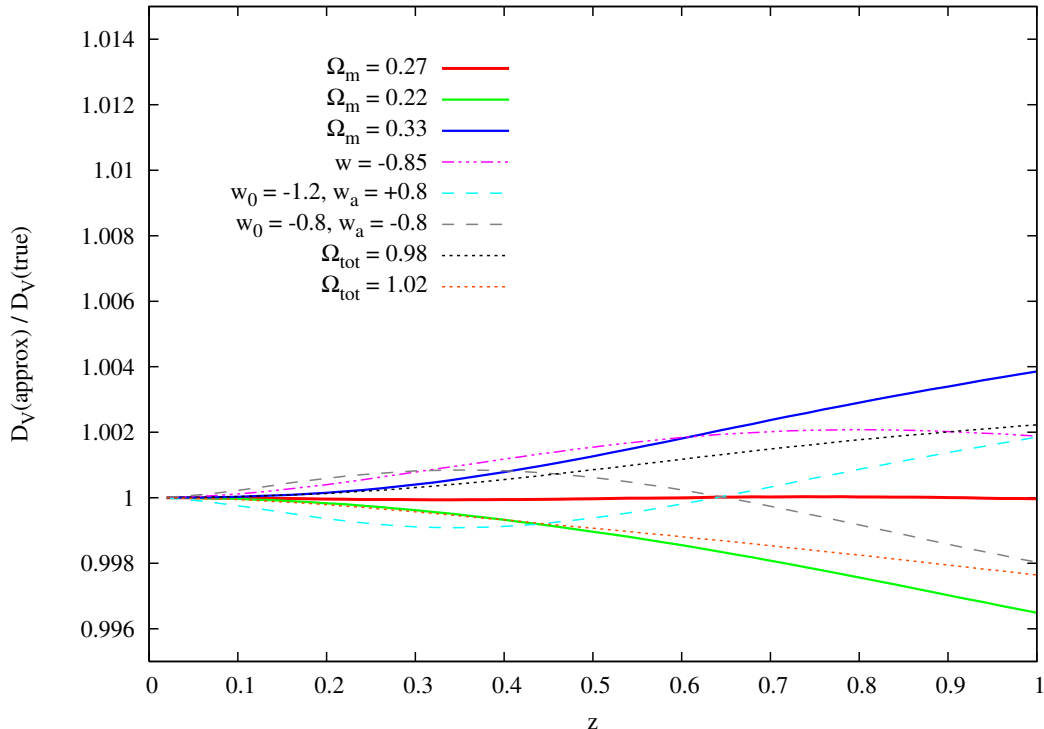


Figure 3. This figure shows the relative accuracy of approximation 8 for various cosmological models, roughly consistent with WMAP. The solid lines show flat Λ CDM models with $\Omega_m = 0.22, 0.27, 0.33$ (bottom to top). The dash-dotted line shows flat w CDM with constant $w = -0.85$; the dashed lines show evolving- w models with values $(w_0, w_a) = (-1.2, +0.8)$ and $(-0.8, -0.8)$ respectively. The dotted lines show non-flat Λ CDM with $\Omega_{tot} = 0.98$ (upper) and 1.02 (lower). (Note the axis scales are different from Figure 2).

nificantly help. Conversely if a bottom-up measurement of r_s does agree at the $\sim 1-2$ percent level with the CMB prediction, this would provide simple and compelling support for the standard set of early-universe assumptions.

We next discuss some questions in both the CMB and local methods for measuring r_s .

4 NON-STANDARD RADIATION DENSITY

Here we consider the effect of non-standard radiation density, which is an important degeneracy for all CMB-determined length scales. This is moderately well-known, first analysed for the BAO case by Eisenstein & White (2004), and also in e.g. de Bernardis et al (2008), but we give a slightly different and hopefully more intuitive explanation compared to previous work.

4.1 Definitions of radiation density

The value of $r_s(z_d)$ is given from the WMAP data alone as 153 Mpc with 2 percent precision, just assuming standard radiation content but no assumptions about flatness or dark energy. However, if the assumption of standard radiation content is dropped, the precision degrades radically to $> 10\%$ (Komatsu et al 2011). The reason is mainly the strong degeneracy between matter density ω_m and radiation density ω_{rad} in the CMB fits: the first three CMB peaks determine the redshift of matter/radiation equality z_{eq} well, with $1 + z_{\text{eq}} \equiv \omega_m/\omega_{\text{rad}} \approx 3200 \pm 140$, but converting to the physical matter density ω_m then relies on an assumption of the total radiation density.

The radiation density is conventionally parametrised by an effective number of neutrino species N_{eff} in the CMB era, defined via

$$\omega_{\text{rad}} \equiv \omega_\gamma \left[1 + \frac{7}{8} \left(\frac{4}{11} \right)^{4/3} N_{\text{eff}} \right] \quad (9)$$

(Here for non-negligible neutrino mass, ω_{rad} is not the present-day radiation density, but the value at z_{eq} rescaled by $(1 + z_{\text{eq}})^{-4}$. We set $\omega_m = \omega_c + \omega_b$ to include dark matter and baryons only, excluding any low-redshift contribution from neutrino mass).

Most analyses assume a standard value very close to $N_{\text{eff}} = 3.046$ effective neutrino species (Mangano et al 2005) which gives $\omega_{\text{rad}} = 1.6918 \omega_\gamma$; and the photon density $\omega_\gamma = (40440)^{-1}$ is set by the very accurate CMB temperature, $T_0 = 2.7255$ K. However, we note that there already some hints of a higher value of N_{eff} from e.g. Keisler et al (2011); these are not yet decisive, but are very interesting.

For general N_{eff} , the above can be rearranged into

$$\omega_m = 0.1339 \left(\frac{1 + z_{\text{eq}}}{3201} \right) [1 + 0.134(N_{\text{eff}} - 3.046)] \quad (10)$$

4.2 The N_{eff} /scale degeneracy

Here we review in more detail the effect of non-standard N_{eff} on cosmological parameter estimates, and show essentially that this creates a degeneracy in overall scale factor which affects all cosmic distances, times and densities, but has very little effect on dimensionless ratios.

It is helpful to rearrange the expression for the sound

horizon (e.g. Eq.6 of Eisenstein & Hu (1998)) in terms of z_{eq} , ω_{rad} and ω_b as the input parameters, which gives

$$r_s(z_d) = 2998 \text{ Mpc} \frac{2}{\sqrt{3}} \omega_{\text{rad}}^{-1/2} (1 + z_{\text{eq}})^{-1} R_{\text{eq}}^{-1/2} \times \ln \left(\frac{\sqrt{1 + R_d} + \sqrt{R_d + R_{\text{eq}}}}{1 + \sqrt{R_{\text{eq}}}} \right) \quad (11)$$

where $R(z) \approx 30330 \omega_b/(1 + z)$ is the baryon/photon momentum density ratio, and R_d , R_{eq} are the values at z_d , z_{eq} respectively. This shows that if we vary ω_{rad} while holding z_{eq} , z_d , and ω_b all fixed, the sound horizon scales simply $\propto \omega_{\text{rad}}^{-1/2}$. In more detail, the WMAP best-fit values show small changes in z_d and ω_b with varying N_{eff} , see Sec 4.7 of Komatsu et al (2011) for details: however, the consequential shifts in $r_s(z_d)$ are some $10\times$ smaller than the dominant $\omega_{\text{rad}}^{-1/2}$ shift, so we ignore those for simplicity.

Next for illustration we take a specific example of two models, an arbitrary model A with $N_{\text{eff}} = 3.046$ and parameters assumed a good fit to WMAP, and a model B with one extra neutrino species (or equivalent in dark radiation), thus $N_{\text{eff}} = 4.046$ but the same z_{eq} . Thus, model B has both ω_{rad} and ω_m larger by 13.4 percent, while the sound horizon in B is smaller by a factor close to $(1.134)^{-1/2} = 0.939$. This would be severely discrepant with the observed position of the CMB acoustic peaks via the acoustic scale ℓ_* , if either the distance to last-scattering $D_A(z_*)$ or H_0 were held fixed.

However, if we also choose model B to have increased ω_{DE} , ω_k by the same factor of 1.134 above, then via

$$h^2 = \omega_m + \omega_{DE} + \omega_k \quad , \quad (12)$$

model B has H_0 increased by 6.5 percent while all of Ω_m , Ω_{DE} , Ω_{rad} , Ω_k are identical in models A and B. Since the expansion function $E(z) \equiv H(z)/H_0$ depends only on the upper-case Ω values above, $E(z)$ remains unchanged at all redshifts; so **all** cosmic distance(z) and $t(z)$ functions are reduced by $\approx 6\%$ in model B relative to A, but distance *ratios* between any two redshifts (related to BAO and SNIa observables and the CMB acoustic angle) remain unchanged. (We note here that ω_b and ω_γ are assumed unchanged between models A and B, so Ω_b and Ω_b/Ω_m are reduced by 13 percent in model B, but these do not appear separately in the Friedmann equation. The implied value of σ_8 will also be slightly different for model B as shown by WMAP, but we do not consider that here).

What is happening here is simple: apart from ω_b , WMAP mainly constrains dimensionless quantities: especially z_{eq} , the acoustic scale ℓ_* at last scattering z_* , and the shift parameter \mathcal{R} . Also, BAO measurements are intrinsically dimensionless ratios such as $r_s/D_V(z)$, while supernova measurements anchored to the local Hubble flow also give dimensionless ratios, essentially $H_0 D_L(z)/c$ or $D_L(z)/D_L(z = 0.03)$ (while H_0 is degenerate with the standardised SN luminosity). All these above provide precision measurements of the uppercase Ω values and w with no overall scale needed.

But, there are three dimensionful quantities (lengths, times and densities, or combinations of these) in homogeneous cosmology; while there are *two* inter-relations: distances and times are related by the known c , and the Friedmann equation relates densities to expansion rate, via G . This implies that even excellent knowledge of all those di-

dimensionless ratios above is not sufficient to solve for any dimensionful quantity; but adding a measurement of *any one* cosmological length, time, or absolute density of matter, radiation or dark energy (in SI units or equivalent) would be sufficient to constrain all the others. Usually, this dimensionful quantity is (implicitly) set by assuming $N_{\text{eff}} \approx 3.046$, which fixes ω_{rad} and thus all the other scales: but if this assumption is dropped, then WMAP+BAO+SNe observations leave us short by one dimensionful quantity, and the N_{eff} vs H_0 degeneracy appears.

Given the above, it is convenient to define the scaled radiation density as

$$X_{\text{rad}} \equiv \omega_{\text{rad}}/1.692 \omega_\gamma = 1 + 0.134(N_{\text{eff}} - 3.046) \quad (13)$$

so that the standard value is 1; and also to choose a fundamental parameter set including

$$\Omega_m ; z_{\text{eq}} ; X_{\text{rad}} ; \omega_b \quad (14)$$

plus optional parameters Ω_k , w defaulting to 0, -1 ; as usual $\Omega_{DE} = 1 - \Omega_m - \Omega_k$. This set couples very naturally to the observables, and turns both ω_m and H_0 into derived parameters, via

$$\begin{aligned} \omega_{\text{rad}} &= X_{\text{rad}}/23904 \\ \omega_m &= (1 + z_{\text{eq}})X_{\text{rad}}/23904 \\ h &\equiv \sqrt{\omega_m/\Omega_m} \end{aligned} \quad (15)$$

Currently, the observational uncertainty on X_{rad} is substantially larger than on the other major parameters: the central value depends somewhat on choice of datasets, with some datasets favouring $N_{\text{eff}} \approx 4$ (e.g. Keisler et al 2011), while others prefer the standard $N_{\text{eff}} \approx 3$ (e.g. Mangano & Serpico 2011). There is broad agreement that $2 \leq N_{\text{eff}} \leq 5$, which maps to $0.86 \leq X_{\text{rad}} \leq 1.27$. We find from WMAP results that if we allow $X_{\text{rad}} \neq 1$, then current cosmological measurements mainly constrain the combinations $\omega_m \approx (0.135 \pm 0.005) X_{\text{rad}}$, $r_s \approx (153 \pm 2)/\sqrt{X_{\text{rad}}}$ Mpc, $H_0 \approx (70 \pm 1.5)\sqrt{X_{\text{rad}}}$ km s $^{-1}$ Mpc $^{-1}$ and $t_0 \approx (13.75 \pm 0.1)/\sqrt{X_{\text{rad}}}$ Gyr; all these dimensionful observables have error bars dominated by the uncertainty in X_{rad} , while most dimensionless ratios are nearly uncorrelated with X_{rad} (the main exceptions are n_s and σ_8 , which both show small positive correlations with X_{rad}). This simple scaling accurately reproduces the degeneracy track of t_0 vs N_{eff} shown by de Bernardis et al (2008).

(We emphasise an important distinction that h and ω_i do *not* count as dimensionless in this discussion; they are clearly pure numbers, but they represent dimensionful quantities rescaled by an arbitrary choice of $H_0 = 100$ km s $^{-1}$ Mpc $^{-1}$ and a fiducial density $\rho_{\text{fid}} = 1.878 \times 10^{-26}$ kg m $^{-3}$. The true dimensionless quantities such as z_{eq} , Ω_m , $H_0 D_A(z)/c$, $H_0 r_s/c$, ℓ_* , $H_0 t_0$, etc, have values independent of any system of units).

To break the above degeneracy, it is sufficient to get an accurate measurement of *any one* dimensionful observable such as H_0 , t_0 , r_s or an absolute distance $D_L(z)$ to any redshift. (A purely local measurement of ω_{rad} , ω_m or ω_{DE} would also suffice, but appears impossible). Other possibilities include the CMB damping tail (see below) at $\ell > 1000$, which brings in the Silk damping length as a new dimensionful quantity which has different scaling with X_{rad} .

Of the various dimensionful parameters above, H_0 is

clearly the most familiar from history, but to constrain N_{eff} it is actually preferable to measure r_s : because $r_s \sqrt{X_{\text{rad}}}$ is well constrained by CMB data alone, independent of late-time dark energy and curvature. In contrast, $H_0/\sqrt{X_{\text{rad}}}$ is well constrained by WMAP+BAO data *if we assume* flatness and $w = -1$, but the constraints become significantly worse if we allow curvature and/or arbitrary dark energy evolution. Therefore, measuring the absolute length r_s is the best route to probe N_{eff} and the early Universe; while combining CMB data with an accurate local H_0 measurement mainly constrains one degenerate combination of N_{eff} , w and Ω_k .

To illustrate this more clearly, the concordance model values of $H_0 \approx 70.5$ km s $^{-1}$ Mpc $^{-1}$ and $r_s \approx 153$ Mpc shift to ≈ 75 km s $^{-1}$ Mpc $^{-1}$ and 144 Mpc respectively if we assume Λ CDM with $N_{\text{eff}} \approx 4.0$. If the latter is the actual cosmology, an observed lower bound $H_0 \geq 73$ km s $^{-1}$ Mpc $^{-1}$ could be fitted with any of $N_{\text{eff}} \approx 4$, or $N_{\text{eff}} \approx 3$ with $w < -1$ and/or open curvature; but a direct upper bound $r_s \leq 148$ Mpc would exclude all of the currently allowed range for $N_{\text{eff}} \approx 3$, and decisively *require* extra radiation or some other new physics at $z > 1000$.

Also, it is helpful to compare the N_{eff} /scale degeneracy to the better-known geometrical degeneracy affecting parameter fitting from the CMB alone (Efstathiou & Bond 1999). Although both degeneracies affect H_0 , the geometrical degeneracy involves holding fixed physical densities of both matter and radiation (thus fixed r_s), while trading off two of Ω_m , Ω_k , w so as to maintain a fixed angular distance to last-scattering $D_A(z_*)$; this is well broken by BAO ratios, as we see below. The N_{eff} /scale degeneracy above also holds z_{eq} fixed, but rescales densities and distances by X_{rad} and $1/\sqrt{X_{\text{rad}}}$ respectively; here both $D_A(z_*)$ and $r_s(z_*)$ shift by a common factor. This N_{eff} /scale degeneracy is *not* broken by BAO distance-ratios, but is broken with an *absolute* BAO length measurement. Therefore, these two degeneracies are “orthogonal” concerning r_s , but get mixed in H_0 , which explains why r_s is a cleaner test of the early Universe.

4.3 An easy route to Ω_m

Here we find a strikingly simple route to Ω_m , accurate to better than 1 percent: first it is convenient to define

$$1 + \epsilon_V(z; \Omega_m, \Omega_k, w) \equiv \frac{cz}{H(\frac{2}{3}z) D_V(z)} \quad (16)$$

so the function ϵ_V is defined to be the (small) correction to approximation (6), as shown in Figure 1. Then, taking an observed BAO ratio $r_s/D_V(z)$, substituting Eq. 11 and using $h/\sqrt{\omega_{\text{rad}}} \equiv \sqrt{(1 + z_{\text{eq}})/\Omega_m}$, we obtain

$$\begin{aligned} \frac{z r_s}{D_V(z)} &= \frac{r_s H(\frac{2}{3}z)}{c} (1 + \epsilon_V) \\ &= (1 + \epsilon_V) \frac{E(\frac{2}{3}z)}{\sqrt{\Omega_m}} \frac{2}{\sqrt{3}} (1 + z_{\text{eq}})^{-1/2} R_{\text{eq}}^{-1/2} \\ &\quad \times \ln \left(\frac{\sqrt{1 + R_d} + \sqrt{R_d + R_{\text{eq}}}}{1 + \sqrt{R_{\text{eq}}}} \right). \end{aligned} \quad (17)$$

This is exact apart from non-linear shifts of r_s . All the terms above are clearly dimensionless: both H_0 and ω_{rad} have can-

celled, and there is only a small implicit dependence on ω_{rad} via very small changes in z_d .

The last three factors on the RHS above are well constrained given only z_{eq} and ω_b from WMAP, which are almost independent of dark energy, curvature or radiation density. Adopting $\omega_b = 0.0225$, the RHS above is very well approximated by

$$\frac{z r_s}{D_V(z)} \simeq 0.01868 (1 + \epsilon_V) \frac{E(\frac{2}{3}z)}{\sqrt{\Omega_m}} \left(\frac{1 + z_{\text{eq}}}{3201} \right)^{0.25}; \quad (18)$$

with the uncertainty due to ω_b below 0.4 percent.

A precise moderate-redshift BAO measurement from SDSS is given by Padmanabhan et al (2012) as $D_V(z = 0.35)/r_s = 8.88 \pm 0.17$; thus the LHS above is 0.0394 ± 0.0008 . This, together with $z_{\text{eq}} \approx 3200 \pm 130$ and neglecting the sub-percent ϵ_V term gives $E(0.233)/\sqrt{\Omega_m} = 2.11 \pm 0.05$; simply squaring this and rearranging gives a linear relation (for $w = -1$) of $\Omega_m = (0.280 + 0.145 \Omega_k)(1 \pm 0.05)$, in excellent agreement with the full likelihood results.

There is a common rule-of-thumb that ‘‘CMB measures ω_m and the BAOs measure H_0 ’’; we see from the above that this is *only* valid assuming the standard $N_{\text{eff}} \simeq 3.0$. For general radiation density, the CMB is really measuring z_{eq} , not ω_m : adding a low-redshift BAO measurement then measures primarily Ω_m , with a small sensitivity to Ω_k and w creeping in via the $E(2z/3)$ term. Combining z_{eq} and Ω_m gives us a value for $H_0/\sqrt{X_{\text{rad}}}$ from Eq. (15), again with mild dependence on Ω_k, w , but does not give an absolute scale.

(The additional information from the large-scale bend in the galaxy power spectrum is discussed in Appendix B).

5 DISTANCE AND SOUND HORIZON MEASUREMENTS

Here we discuss some considerations on observational issues and the realistic precision available for measurements of the absolute BAO length, both locally and from future CMB measurements.

5.1 Distance ladder measurements

Given a measurement of $r_s/D_V(z)$ from BAOs in a redshift survey, we need an absolute measurement of $D_L(4z/3)$ to apply Eq. 8 and obtain an absolute measurement of r_s independent of the CMB. The most obvious route to measure $D_L(4z/3)$ is to combine a local distance-ladder measurement of H_0 with a large sample of type-Ia supernovae centred at redshift near $4z/3$ to measure $D_L(4z/3)$; along with approximation 8 this provides a direct calibration of $D_V(z)$ and thus r_s .

Doing this at fairly low redshift has several advantages: firstly, it is observationally much cheaper to accumulate a large sample of supernovae at $z \lesssim 0.3$ compared with $z \gtrsim 0.5$, and such a sample should arise naturally from the ongoing PanSTARRS Medium Deep Survey (Kaiser et al 2010) and the Dark Energy Survey (Bernstein et al 2012). Also, lower redshift provides a smaller lever-arm for possible time evolution of the mean supernova brightness, minimising systematic errors. Given an overabundance of supernovae (e.g. several hundred in the relevant redshift bin), one can

afford to subdivide the sample by lightcurve stretch, host galaxy type etc, to provide consistency checks.

Also, there is growing evidence that SNe Ia are closest to standard candles in the rest-frame near-IR wavelengths, specifically the J and H passbands (Barone-Nugent et al 2012). At $z \approx 0.3$ these bands redshift into observed H and K_s respectively, so that redshift is a sweet-spot which minimises k-corrections.

We note here that this is significantly different to the more common case of computing dark energy figures of merit; in the dark energy case, breaking degeneracies between Ω_m, Ω_k and dark energy parameters w_0, w_a requires relative distance measurements spanning a broad range of redshift $0.2 \lesssim z \lesssim 1.5$; for supernovae anchored to local samples at $z \sim 0.05$, SNe at higher redshift have greater leverage on w_0 and especially w_a . Since BAOs are anchored in the CMB, the preference for higher redshift is weaker than for SNe, but the rapid increase in available cosmic volume still favours redshifts $0.5 \lesssim z \lesssim 1.5$ for precision measurements of w_0 and w_a (Weinberg et al 2012).

In contrast to the above, for an absolute r_s measurement we only need to measure an absolute distance D_L to one specific redshift matched to a given BAO survey; the overall r_s accuracy is simply the quadrature sum of the BAO and D_L errors, with a small addition from the error in Eq. 8, but there is no lever-arm gain towards higher redshift. Thus, the number of required SNe for given precision on D_L is independent of the target redshift; thus low redshifts are both observationally cheaper, and more robust against systematics such as time evolution and imperfect k -corrections.

5.2 Physical distance measurements

One major benefit of our approximation 8 is that there is *no explicit dependence* on H_0 . Therefore, if we can measure $D_L(z)$ to $z \sim 0.25$ using some physical-based method which does not rely on calibration via the local distance ladder and H_0 , we automatically bypass the uncertainties in the local distance scale.

There are several current or proposed methods for doing this, including gravitational lens time-delays, Sunyaev-Zeldovich measurements of galaxy clusters, and the expanding-photosphere method applied to Type-II supernovae; however, all of these methods have some level of model dependence and it is not yet clear whether they can reach the percent level absolute accuracy (e.g. 2 percent accuracy for a 3σ detection of one additional neutrino species). The lens time-delay method is especially clear at low lens redshift; while lensing observables involve a combination of lens and source distances D_l, D_{ls} and D_s , selecting systems with $z_l \ll z_s$ makes the ratio D_{ls}/D_s close to unity and well constrained, which is favourable for absolute measurement of the lens distance.

Potentially the ultimate D_L calibration method is the detection of gravitational waves from coalescing compact binaries (Schutz 1986), since the model waveforms can be predicted extremely precisely assuming only Einstein gravity, and the method is completely immune to dust extinction or astrophysical nuisance parameters. Of course, such events have not been directly observed so far, but the observations of binary pulsars (Kramer & Stairs 2008) leave no doubt that the waves exist, and there are ongoing upgrades to Ad-

vanced LIGO and VIRGO which should give a near-certain detection of binary inspirals around 2015, assuming they reach their design sensitivity.

These second-generation GW experiments will probably provide only modest D_L accuracy for most events; however, if we are lucky there may be a few “golden events” with high signal to noise, such as massive black hole events at $z \sim 0.1$. In the longer term, there is an ongoing design study for a third-generation ground-based gravitational wave observatory called “Einstein Telescope” (Sathyaprakash et al 2011) for the post–2025 era; this is projected to detect binary neutron-star mergers to $z \sim 2$, and neutron-star + black hole mergers to $z \sim 4$. For the closest merger events at $z \sim 0.1 - 0.2$, Einstein Telescope would provide very high SNR and percent-level absolute accuracy on D_L for each event. If these can be tied to a unique galaxy, or statistically tied to a given cluster or sheet of galaxies, redshift constraints will be quite precise.

The future of GW distance measurements is naturally quite uncertain: however, one feature is generic: since the method is largely limited by instrumental SNR not astrophysical scatter, the closest GW inspirals should always provide the best distance precision per event. Furthermore, the closer inspirals lead to much smaller position error ellipsoids, and make it much easier to identify an optical counterpart, or statistically identify the host galaxy in a group or cluster. (Assuming the relative distance and angular errors for a GW inspiral scale $\propto 1/\text{SNR}$, then the comoving volume of the GW error box scales approximately as D^3 ; this results in fewer candidate host galaxies per burst at low redshift, by a very steep factor).

From the above discussion, it is quite generic that for any cosmological distance estimate, the best prospects for percent-level absolute accuracy on $D_L(z)$ tend to occur at modest redshift $0.1 \lesssim z \lesssim 0.25$: this is distant enough for galaxy peculiar velocities to be a small effect, but close enough to give high signal/noise ratio and minimal nuisances from possible time evolution and uncorrectable gravitational lensing effects. Until the distant future when we can get cosmological distance measurements with significantly better than 1 percent absolute accuracy, then a low redshift will be preferred for anchoring the absolute BAO length.

5.3 Planck measurement of r_s

In the near future, Planck data is expected to improve the precision on z_{eq} to around 1 percent; assuming all the “standard” early universe conditions (i.e. GR, standard radiation with $N_{\text{eff}} = 3.046$, negligible early dark energy, etc), this will determine the sound horizon to ~ 0.3 percent precision, which is significantly better than any foreseen direct distance measurement. So, why bother measuring r_s locally?

If instead N_{eff} is treated as free, Planck will still measure $r_s \sqrt{X_{\text{rad}}}$ to 0.3 percent, but the error on X_{rad} will dominate: the Planck measurements of the CMB damping tail (peaks 4,5,6) will provide a useful constraint on N_{eff} , but a plausible uncertainty of ≈ 0.3 in N_{eff} from Planck is equivalent to 4 percent in X_{rad} and 2 percent in r_s ; this is around $6\times$ worse than the standard-radiation case, and moderate-redshift BAO and distance measurements can potentially be competitive or better than this accuracy.

Furthermore, the fitting of the radiation density from the CMB relies on fairly subtle and smooth suppression of power in the CMB damping tail (Bashinsky & Seljak 2004; Hou et al 2012); this effect is significantly degenerate with other possible adjustable parameters, including changes in primordial Helium abundance Y_p and non-zero running of the primordial spectral index $dn_s/d\ln k$ (Hou et al 2012), (and also with possible experimental systematics such as imperfect modelling of beam sidelobes). In CMB analyses, N_{eff} , Y_p and $dn_s/d\ln k$ are generally fitted one-at-a-time with the other two fixed to “standard” values; however, if two or three of these are simultaneously free, the CMB-only constraints on $r_s(z_d)$ may well be significantly worse than 2 percent; while the local BAO route above can provide a direct measure of r_s which is practically theory-independent.

Therefore, although cosmic variance means that local BAO measurements cannot compete with the 0.3 percent best-case Planck precision on r_s , this is not a major drawback: a local measurement of r_s to 1–2 percent absolute accuracy would still be of major benefit for cosmology, and could detect or exclude various early-universe effects such as non-standard N_{eff} with high significance; this method is independent of early-universe uncertainties including Y_p and spectral index running which may potentially hamper the Planck measurement of N_{eff} .

Another motivation is that the value of N_{eff} from the CMB is somewhat degenerate with the primordial spectral index n_s and $dn_s/d\ln k$ (e.g. Hou et al 2012): this can have major implications for constraining the early universe and inflation theory. If N_{eff} is fixed to 4.04 rather than the standard value 3.04, the WMAP best-fit value of n_s moves up from ≈ 0.96 to ≈ 0.975 to compensate; this is a small change, but is potentially very important because the scale-invariant value of 1.00 is then no longer ruled out at high significance. A constraint on N_{eff} directly from the absolute length r_s is almost independent of the primordial power spectrum, and is therefore extremely valuable.

In principle we can achieve better precision by going to a higher redshift BAO survey to reduce cosmic variance, e.g. Euclid should measure the transverse BAO angle $r_s/D_A(z)$ to better than 0.4 percent in many bins between $0.7 \leq z \leq 1.7$ (Laureijs et al 2011). Adding a 0.4 percent distance measurement to a matching redshift, this could measure N_{eff} to around ± 0.1 precision, which is substantially better than Planck. However, a sub-percent absolute distance to such a redshift currently appears extremely challenging given the potential systematics: thus the low-redshift route outlined above remains a promising intermediate step.

5.4 An ultimate BAO survey at $z \sim 0.2$

The considerations above on distance measurements and CMB degeneracies provide a very strong motivation for obtaining the best possible BAO measurements at modest $z \sim 0.2$, approaching the cosmic variance limit. The ongoing BOSS project is a large step in this direction, but there are several potential improvements: firstly of course BOSS only covers around 1/4 of the entire sky, so adding coverage of the Southern hemisphere is very useful; secondly, sampling a somewhat higher space density of galaxies can improve reconstruction of the BAO peak, and thirdly we may ex-

pand the survey to lower galactic latitudes for maximal sky coverage.

Until recently, galaxy surveys have disfavoured low galactic latitudes due to both extinction problems and increased stellar contamination (e.g. from blended images which are hard to morphologically classify). However, the recently completed WISE mid-IR survey combined with the ongoing VISTA Hemisphere Survey should provide a galaxy sample of ample depth, and minimal sensitivity to galactic extinction which could push down to $|b| \sim 15^\circ$. Availability of optical+near-IR colours can also greatly improve the star-galaxy separation, so stellar contamination should remain manageable. The cosmic-variance limits on BAO measurements have been calculated by Seo & Eisenstein (2007); for 3/4 of the full sky and realistic reconstruction methods, interpolation from their Figure 3 predicts precision ≈ 1.2 percent on $r_s/D_V(z = 0.2)$; this accuracy is similar to optimistic projections for local H_0 measurements. Such a BAO survey is comfortably within reach of proposed high-multiplex multi-object spectrographs such as 4MOST on the VISTA telescope, or DESpec at CTIO. The required area is very large, but the target density ~ 50 galaxies per deg^2 is rather low, so such an observing program would only take a modest fraction of the total number of fibres, and could be run in a simultaneous mode in parallel with stellar and other surveys.

Furthermore, an accurate low-redshift BAO measurement, when compared to a radial BAO measurement at $z \sim 0.7$, can provide a clean smoking-gun test of cosmic acceleration entirely from the two BAO measurements (Sutherland 2012); that test is independent of supernovae, CMB data and general relativity. BAO measurements at $z \gtrsim 0.5$ are necessary but not sufficient for this test, since very little acceleration happened earlier than $z = 0.5$.

6 CONCLUSION

Measuring the absolute rather than relative BAO length scale forms a powerful test of standard early-universe cosmology, especially probing the radiation density along with other possible non-standard effects at $z > 1000$.

As a step in this direction, we have found a simple and highly accurate approximation (Eq. 8) relating the BAO dilation scale $D_V(z)$ to the luminosity distance D_L at a slightly higher redshift. This is accurate to ≤ 0.2 percent at $z \leq 0.4$ for all plausible WMAP-compatible Friedmann models, including modest curvature and time-varying dark energy; the inaccuracy is substantially smaller than the cosmic variance limit for low-redshift BAO measurements. The approximation does not explicitly depend on H_0 , so remains applicable if there is any direct physics-based measurement of $D_L(z)$ bypassing the local distance ladder. The only ways for Eq. 8 to have percent-level errors are very radical, such as violation of the distance-duality relation $D_L = (1+z)^2 D_A$, or a sharp phase transition in dark energy at low redshift, e.g. a sharp jump in $w(z)$ causing a kink feature in $H(z)$.

We also reviewed the degeneracy between radiation density and cosmic scales, and showed this is close to a rescaling of all dimensional observables (except baryon and photon densities), while leaving most dimensionless ratios unchanged.

Given realistic future observations, the approximation above can provide a high-precision calibration of the BAO length scale using only low redshift data, which in turn provides a powerful test of standard $z > 1000$ CMB assumptions, and in particular a robust test of the radiation density independent of the CMB damping tail.

A measurement of H_0 is also useful, but on its own does not fully break degeneracies: e.g. a high-precision measurement of H_0 significantly greater than $73 \text{ km s}^{-1} \text{ Mpc}^{-1}$ would signal a problem for vanilla Λ CDM, but could indicate any one of $w < -1$, weak open curvature or increased radiation density, and without an absolute r_s measurement it would be hard to discriminate these. In contrast, an absolute BAO length measurement can cleanly detect or constrain non-standard pre-CMB physics, almost independent of late-time effects such as $w \neq -1$ or weak curvature, and with minimal degeneracy with n_s and running spectral index. This may also be important for inflation theory, since the currently strong evidence for $n_s < 1$ becomes substantially weaker if N_{eff} is larger than the standard value.

We can essentially distinguish two possibilities: if all the standard CMB assumptions are correct, then Planck will determine $r_s(z_d)$ better than the cosmic variance on the BAO length: then an absolute BAO length measurement essentially provides a strong null test of the standard cosmology at around 1-2 percent precision, but does not improve our error bars on Ω_m , w etc.

However, if one or more of the standard early-universe assumptions is wrong, this can be absorbed into biased values of H_0 , and to a lesser extent Ω_m and w , in joint fits to CMB, BAO, and supernova data alone. Therefore, a direct low-redshift measurement of r_s can be very powerful for discriminating early-universe modifications such as extra radiation or early dark energy, from late-time effects such as dark energy $w \neq -1$ or small non-zero curvature.

ACKNOWLEDGEMENTS

I thank Will Percival for helpful discussions, and Roelof de Jong and the 4MOST science team for information on survey strategies. I acknowledge the use of WMAP data from the Legacy Archive for Microwave Background Data Analysis (LAMBDA) at GSFC (lambda.gsfc.nasa.gov), supported by the NASA Office of Space Science.

(The definitive version of this paper is available in MNRAS at DOI:10.1111/j.1365-2966.2012.21666.x)

REFERENCES

- Ade, P.A.R. et al (Planck Collaboration), 2011, *A&A*, 536, 1.
- Alam U., Sahni V., Saini T-D., Starobinsky A.A., 2003, *MNRAS*, 344, 1057.
- Barone-Nugent R.L. et al, 2012, arXiv.org/1204.2308
- Bashinsky S. & Seljak U., 2004, *Phys. Rev. D*, 69, 083002.
- Bassett B.A. & Hlozek R., 2010, in “Dark Energy”, ed P. Ruiz-Lapuente, p246, Cambridge Univ. Press, Cambridge.
- Bernstein J.P., Kessler R., Kuhlmann S. et al 2012, *ApJ*, 753, 152.
- Beutler F., Blake C., Colless M. et al, 2011, *MNRAS*, 416, 3017.
- Blake C. & Glazebrook K., 2003, *ApJ*, 594, 665.
- Blake C., Davis T., Poole G. et al, 2011, *MNRAS*, 415, 2892.
- Bond J.R., Efstathiou G., 1984, *ApJ*, 285, L45
- Cole S., Percival W.J., Peacock J.A. et al, 2005, *MNRAS*, 362, 505.
- de Bernardis F., Melchiorri A., Verde L., Jimenez R., 2008, *JCAP*, 03, 020.
- Efstathiou G., Bond J.R., 1999, *MNRAS*, 304, 75.
- Efstathiou G., Sutherland W., Maddox S., 1990, *Nature*, 348, 705.
- Eisenstein D.J. & Hu W., 1998, *ApJ*, 496, 605.
- Eisenstein D.J., White M., 2004, *Phys.Rev.D*, 70, 103523.
- Eisenstein D.J., Zehavi I., Hogg D. et al, 2005, *ApJ*, 633, 560.
- Eisenstein D.J, Seo H., Sirko E., Spergel D.N., 2007, *ApJ*, 664, 675.
- Eisenstein D.J, Seo H., White M., 2007, *ApJ*, 664, 660.
- Hou Z., Keisler R., Knox L., Millea M., Reichardt C., 2011, arXiv.org/1104.2333
- Kaiser N., Burgett W., Chambers K. et al, 2010, *Proc. SPIE*, 7733, 12.
- Keisler R., Reichardt C.L., Aird K.A. et al, 2011, *ApJ*, 743, 28.
- Komatsu E., Smith K., Dunkley J. et al, 2011, *ApJS*, 192, 18.
- Kramer M., Stairs I.H., 2008, *ARA&A*, 46, 541.
- Laureijs, R. et al, 2011, *Euclid Red Book*, arXiv.org/abs/1110.3193
- Linder E., Robbers G., 2008, *JCAP*, 06, 004.
- Mangano G., Miele G., Pastor S., Pinto T., Pisanti O., Serpico P.D., 2005, *Nucl. Phys. B*, 729, 221.
- Mangano G., Serpico P.D., 2011, *Phys. Lett. B*, 701, 296.
- Meiksin A., White M. & Peacock J.A., 1999, *MNRAS*, 304, 851.
- Menegoni E., Archidiacono M., Calabrese E. et al, 2012, *Phys. Rev. D*, 85, 107301.
- Peebles P.J.E. & Yu J.T, 1970, *ApJ*, 162, 815.
- Padmanabhan N., Xu X., Eisenstein D.J., Scalzo R., Cuesta A.J., Mehta K.T., Kazin E., 2012, arXiv.org/1202.0090
- Percival W.J., Sutherland W., Peacock J.A. et al, 2002, *MNRAS*, 337, 1068.
- Percival W.J., Reid B.A., Eisenstein D.J. et al, 2010, *MNRAS*, 401, 2148.
- Reid B.A., Percival W.J., Eisenstein D.J. et al, 2010, *MNRAS*, 404, 60.
- Sathyaprakash B., Abernathy M., Acernese F. et al, 2011, arXiv.org/1108.1423
- Schutz B.F., 1986, *Nature*, 323, 310.
- Seo H-J., Eisenstein D.J., 2003, *ApJ*, 598, 720.
- Seo H-J., Eisenstein D.J., 2007, *ApJ*, 665, 14.
- Seo H-J. et al, 2012, arXiv.org/1201.2172.
- Seo H-J., Eckel J., Eisenstein D.J. et al, 2010, *ApJ*, 720, 1650.
- Seo H-J., Siegel E.R., Eisenstein D.J., White M., 2008, *ApJ*, 686, 13.
- Stern D., Jimenez R., Verde L., Kamionkowski M., Stanford S.A., 2010, *JCAP*, 02, 008.
- Sutherland W., 2012, *MNRAS*, 420, 3026. (arXiv.org/abs/1105.3838)
- Weinberg D.H., Mortonson M.J., Eisenstein D.J., Hirata C., Reiss A.G., Rozo E., 2012, *Phys. Reports*, submitted (arXiv.org/1201.2434)
- White M., Blanton M., Bolton A. et al, 2011, *ApJ*, 728, 126.
- Zunckel C., Okouma P., Muya Kasanda S., Moodley K, Bassett B.A., 2011, *Phys.Lett.B*, 696, 433.

APPENDIX A: THE TAYLOR SERIES FOR D_V

Here we derive the Taylor series for $D_V(z)$ and approximation 7; these are not used in the main part of the paper, but are useful to provide an analytic understanding of the high accuracy of approximations (7) and (8), and the dependence on cosmological parameters.

We start by defining the usual deceleration parameter q and the jerk parameter j (e.g. Alam et al 2003) as

$$q \equiv -\frac{d^2 a/dt^2}{aH^2}, \quad j \equiv \frac{d^3 a/dt^3}{aH^3}. \quad (\text{A1})$$

We can rearrange these in terms of d/dz , and using the chain rule we find

$$\frac{d}{dz} \left(\frac{1}{H} \right) = \frac{1+q}{(1+z)H}, \quad \frac{d^2}{dz^2} \left(\frac{1}{H} \right) = \frac{2+4q+3q^2-j}{(1+z)^2 H}. \quad (\text{A2})$$

Using these, with subscript 0 denoting present-day values, we obtain the series

$$\frac{cz}{H(z)} = \frac{cz}{H_0} \left[1 - (1+q_0)z + \frac{2+4q_0+3q_0^2-j_0}{2} z^2 + \dots \right] \quad (\text{A3})$$

and integrating and including the leading-order curvature term gives

$$(1+z)D_A(z) = \frac{cz}{H_0} \left[1 - \frac{1+q_0}{2}z + \frac{2+4q_0+3q_0^2-j_0+\Omega_k}{6} z^2 + \dots \right] \quad (\text{A4})$$

Inserting the above two expressions into the definition of D_V , collecting powers of z and using $(1+x)^{1/3} = 1+x/3-x^2/9+\dots$, we obtain the Taylor series for D_V as

$$D_V(z) = \frac{cz}{H_0} \left[1 - \frac{2(1+q_0)}{3}z + \frac{19+38q_0+29q_0^2-10j_0+4\Omega_k}{36} z^2 + \dots \right] \quad (\text{A5})$$

(We note that for concordance Λ CDM, the 3-term sum above has error < 0.25 percent at $z < 0.3$, but worsens quite rapidly above this.)

Substituting $4z/3$ in A4, we have

$$\frac{3}{4} \left(1 + \frac{4}{3}z \right) D_A\left(\frac{4}{3}z\right) = \frac{cz}{H_0} \left[1 - \frac{2(1+q_0)}{3}z + \frac{16}{54}(2+4q_0+3q_0^2-j_0+\Omega_k) z^2 + \dots \right] \quad (\text{A6})$$

Comparing the above two equations, it is clear that approximation 7 is correct to second order in z , for any values of cosmological parameters. Subtracting (A5) from (A6) and dividing by (A5), we then find that the ratio of the RHS to LHS of approximation 7 is

$$\frac{3}{4} \frac{(1+\frac{4}{3}z)D_A(\frac{4}{3}z)}{D_V(z)} = 1 + \frac{z^2}{108} \left[\frac{14}{9} - 2j_0 + 9 \left(q_0 + \frac{7}{9} \right)^2 + 20\Omega_k \right] + O(z^3). \quad (\text{A7})$$

A flat Λ CDM model has $q_0 = \frac{3}{2}\Omega_m - 1$ and $j_0 = +1$, hence the term in square brackets above simplifies to $\frac{1}{4}\Omega_m(81\Omega_m - 24)$: this is less than 1 for plausible values of $\Omega_m < 0.4$ (it is -0.16 for the concordance model).

More generally, for conservative ranges of parameters $-1 < q_0 < -0.4$, $0 < j_0 < 2$ and $|\Omega_k| < 0.05$, the square-bracket is not significantly bigger than ± 4 ; with the prefactor of $1/108$, this explains the excellent accuracy of approximation 7 at moderate redshift. This also suggests that approximation 7 should remain fairly accurate for modified-gravity models, as long as they are homogeneous, have weak curvature and q_0, j_0 not very different from the concordance model.

Finally we note that the square-bracket has value 14.25 for an Einstein-de Sitter model, and approximately 22 for a zero- Λ open model, explaining the low-redshift limit of those models shown in Figure 2.

APPENDIX B: LARGE-SCALE STRUCTURE AND z_{eq}

Here we note that while BAO parameter estimates are strongly dependent on correct deduction of z_{eq} from the CMB, the overall shape of the large-scale galaxy power spectrum does provide an independent check of this.

The large-scale galaxy clustering pattern actually contains two key length scales, the BAO length discussed above, and also the “big bend” scale which describes the overall broad-band shape of the galaxy power spectrum $P(k)$ excluding the BAO wiggles; these two are approximately independent observables. Assuming the primordial power spectrum is well described by a power-law, $n_s \sim 0.96$ and the dark matter is cold or warm (not hot), then fitting the “big bend” in a galaxy power spectrum essentially measures the comoving light horizon size r_H at matter-radiation equality, again relative to $D_V(z)$ at the characteristic redshift of the given survey: this gives

$$z \frac{r_H(z_{\text{eq}})}{D_V(z)} = (1 + \epsilon_V) \frac{E(2z/3)}{\sqrt{\Omega_m}} \frac{2(\sqrt{2} - 1)}{\sqrt{(1 + z_{\text{eq}})}}; \quad (\text{B1})$$

which is not explicitly dependent on X_{rad} . For $X_{\text{rad}} = 1$, at small z the above has the well-known scaling $\propto (\Omega_m h)^{-1}$, with a result $\Omega_m h \approx 0.20$ which has remained consistent over many large galaxy surveys, since the first reliable estimate from the APM Galaxy Survey (Efstathiou, Sutherland & Maddox 1990), through 2dFGRS (Percival et al 2002) and SDSS (Reid et al 2010).

We see that the big-bend observable in (B1) has the same $E(2z/3)/\sqrt{\Omega_m}$ factor as the BAO ratio in (18), but has a different dependence on z_{eq} . Taking the ratio of these two characteristic lengths, we have

$$\begin{aligned} \frac{r_s(z_d)}{r_H(z_{\text{eq}})} &\equiv \frac{r_H(z_d)}{r_H(z_{\text{eq}})} \frac{r_s(z_d)}{r_H(z_d)} \\ &\simeq \frac{\left(\frac{1+z_{\text{eq}}}{1+z_d} + 1\right)^{1/2} - 1}{\sqrt{2} - 1} \frac{0.886}{\sqrt{3}}; \end{aligned} \quad (\text{B2})$$

here the second factor $0.886/\sqrt{3}$ represents the weighted average sound speed c_s/c prior to the drag redshift; the given value is for the concordance model, but this term is very insensitive to reasonable parameter variations. The first term above depends only on the ratio $(1 + z_{\text{eq}})/(1 + z_d)$, and scales approximately $\propto (1 + z_{\text{eq}})^{0.75}$ around the concordance model; there is no separate dependence on Ω_m , h and X_{rad} , so this ratio is predicted robustly given just z_{eq} from WMAP alone.

Due to various uncertainties in overall $P(k)$ shape from possible effects such as scale-dependent bias, non-linearity, redshift-space distortions, neutrino masses, running of n_s etc, this BAO/bend ratio seems unlikely to independently measure z_{eq} to a precision comparable to the current 4 percent precision from WMAP, and still less the 1 percent expected from Planck. However, the fact that parameters estimated from CMB+BAO also provide a reasonable fit to the overall $P(k)$ shape provides a valuable consistency check, which the concordance model passes (Reid et al 2010). This strongly argues that the WMAP-only estimate of z_{eq} *cannot* have a gross error from unknown physics, unless there has been a fortuitous cancellation of effects.

The above also shows that measuring $P(k r_s)$ in dimensionless units rescaled by the BAO length may be helpful for testing for neutrino masses or non-standard physics around $z \sim z_{\text{eq}}$, since this is very robust against shifts in Ω_m , H_0 and X_{rad} .

This paper has been typeset from a $\text{\TeX}/\text{\LaTeX}$ file prepared by the author.